Intensity fluctuation spectroscopy of small numbers of dye molecules in a microcavity

S. C. Kitson, P. Jonsson,* J. G. Rarity, and P. R. Tapster
Defence Evaluation and Research Agency, St. Andrews Road, Malvern, Worcestershire WR14 3PS, United Kingdom
(Received 12 January 1998)

The spontaneous emission from a thin layer of a dilute solution of fluorescent dye molecules within an optical microcavity has been studied. Strong fluctuations in fluorescence intensity are observed when the average number of molecules in the measurement volume is small. We have performed experiments that simultaneously characterize these fluctuations over nine orders of magnitude of time, from ns to s. These measurements have identified photon antibunching characteristic of single-molecule emission, along with triplet-state shelving and diffusion driven number fluctuations. The results give fundamental information on the kinetics of dye molecules and allow one to speculate about the prospect of using single molecules as sources of single photons for quantum optics. [S1050-2947(98)00107-3]

PACS number(s): 42.50.Dv, 33.50.−j, 42.55.Sa

I. INTRODUCTION

The advent of relatively efficient single photon detectors has made it possible to study the emission of light from single molecules [1–3]. This allows one to study the properties of single molecules rather than the bulk and can give otherwise unobtainable information on the molecular environment. In this paper we describe measurements of the light emitted from single dye molecules located in a microcavity. The measurements give information on the kinetic processes involved and are aimed at developing this system as a source of single photons.

A reliable and efficient source of single photons is desirable for both basic research into the quantum properties of light, and for applications including quantum computing and quantum cryptography [4]. A single fluorescent molecule or atom is one potential source [5,6] because it can only emit one photon at a time. It then takes a certain characteristic time for the electron to be excited to the upper state before another photon can be emitted. The emitted light is thus antibunched and tends to consist of single photons separated by a time interval determined by the excited-state lifetime and the pumping rate.

In our system the dye molecules are in a thin (40-nm) liquid layer confined within a Fabry-Perot cavity, which serves to increase the efficiency with which the spontaneous emission is collected. The single-molecule regime is reached by using very dilute ($10^{-9}M$) dye solutions and a small illumination volume (around 40 nm thick by 6 μm diameter). The fluorescence signal exhibits strong fluctuations on time scales ranging from ns to s. In this paper we describe a system for measuring these fluctuations over the required nine orders of magnitude of time interval and extract information related to the excited-state lifetime, the triplet lifetime, and the diffusion time.

II. EXPERIMENT

The dye used was Rhodamine 6G (R6G) dissolved in propylene carbonate. Propylene carbonate was chosen as the solvent because of its low intrinsic fluorescence and low volatility. R6G is highly efficient and can be excited with the 488-nm line from an argon ion laser.

The dye solution is placed in a microcavity consisting of two dielectric mirrors, made from alternating layers of silica ($n=1.5$) and tantalum pentoxide ($n=2.265$). The microcavity serves to increase the efficiency with which the spontaneous emission from the dye is collected. The peak reflectivity of the mirrors was designed to be at a wavelength of 560 nm by making the thickness of each layer $\lambda/4n$ (where λ is 560 nm and n is the refractive index of the layer). The top layer of each mirror is silica, deliberately grown 20 nm thinner than the $\lambda/4n$ condition. The microcavity is formed by placing a drop of the dye solution on one mirror, and then pressing the other one on top. Placing the cavity in a vacuum chamber for approximately 1 h causes the liquid to slowly evaporate, pulling the two mirrors together. The resulting structure is a $\lambda/2n$-thick microcavity with a dye layer, approximately 40 nm thick, at the center.

The cavity material is the lower index silica so that the dye layer sits at the antinode of the electric field of the fundamental cavity mode, into which the molecules preferentially emit. This narrows the emission spectrum to match the cavity bandwidth and so increases the efficiency with which the light can be collected through a narrow band pass filter that is used to discriminate the fluorescence from scattered laser light. The narrowing of the emission spectrum can be seen in Fig. 1, which shows the emission spectrum obtained from a microcavity (solid line) and from a sample that does not have the multilayer dielectric mirror coatings, but which is identical in all other respects (broken line).

As well as narrowing the emission spectrum the microcavity also increases the total intensity of the emitted light by a factor of 2, because the structure is designed to only emit light through the top mirror. This is achieved by designing the output mirror (with five pairs of layers) to have around 10% transmission over the range 540–590 nm, while the second mirror (with nine pairs of layers) is highly reflecting (99.9%). The increase in emitted light is evident from the measured spectra in Fig. 1. The area under the curve for the microcavity sample is twice the area under the curve for the sample without the mirrors. Taking into account the collec-

*Present address: KTH-Electrum, Department of Electronics, FMI, Electrum 229, S164 40 Kista, Sweden.

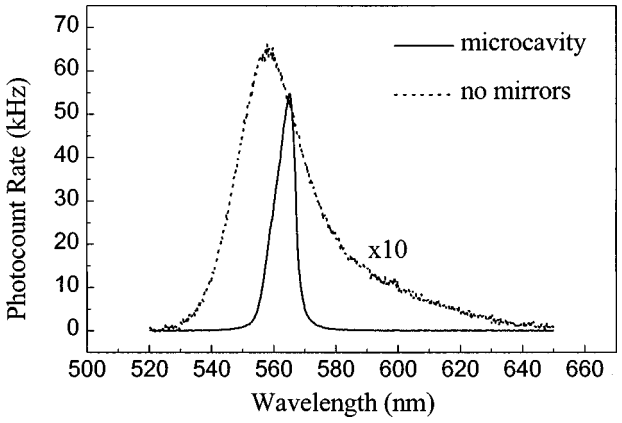

FIG. 1. Fluorescence spectrum of R6G in propylene carbonate measured in the microcavity (solid line) and in a structure without mirrors (broken line). The measurements for the sample without mirrors have been multiplied by a factor of 10 to improve clarity.

tion efficiency of the microcavity, the transmission of the filters used, the reflections at the glass interfaces in the setup, and the quantum efficiency of the detectors, we estimate the photon collection efficiency of our system to be 2×10^{-4}.

Figure 2 is a schematic of the confocal fluorescence microscope used to study the fluorescence from the microcavity. The 488-nm light from a cw argon ion laser is focused through a 100-μm pinhole and then through a microscope objective ($\times$25,0.35 numerical aperture) onto the microcavity. The same lens also collects the fluorescence from the dye molecules. The diameter of the region from which the light is collected is defined by the pinhole to be around 6 μm. The collected light passes through the dichroic mirror and additional filters are used to remove any remaining laser light. The fluorescence light is divided equally between two avalanche diode single photon counting detectors that are connected to a photocount correlator and to a time interval analyzer. Two detectors are used to circumvent the problems associated with the deadtime of the detectors (1 μs), allowing the measurement of time intervals as small as 0.5 ns. The filters in front of the detectors block the transmission of IR, preventing crosstalk between the detectors.

The electronics measures the photocount correlation function [7]

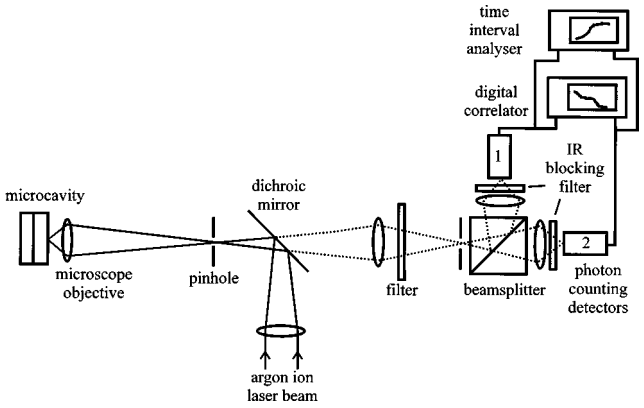

FIG. 2. Schematic of the apparatus used to study the fluorescence fluctuations from a small number of dye molecules in a microcavity.

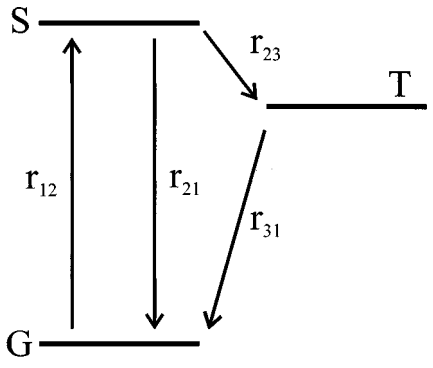

FIG. 3. Schematic energy scheme showing the ground (G), excited singlet (S), and triplet (T) states, and the various transition rates between the states.

$$g_c^{(2)}(t)=\frac{\langle I_{d1}(t_0)I_{d2}(t_0+t)\rangle}{\langle I_{d1}\rangle\langle I_{d2}\rangle}, \tag{1}$$

where $I_{d1}(t_0)$ and $I_{d2}(t_0+t)$ are the recorded photocounts in detectors 1 and 2 at times t_0 and t_0+t, respectively, and the angle brackets denote averages over the start times t_0. It is this function that characterizes the fluctuations in the signal. It can be shown that this measurement is equivalent to a measurement of the normalized autocorrelation function of intensity [8]

$$g^{(2)}(t)=\frac{\langle I(t_0)I(t_0+t)\rangle}{\langle I\rangle^2}\equiv g_c^{(2)}(t), \tag{2}$$

but avoids the short time distortions arising due to detector after pulsing and dead time.

Over the time range 100 ns to 1 s, $g^{(2)}(t)$ is measured using the digital correlator, which samples the photocount in time bins of width T and uses parallel multipliers to evaluate Eq. (1) in real time. The system used here contains eight 32-channel correlators with sample times T,6T,36T,…, etc. with $T=100$ ns.

The time range from 0.5 to 100 ns is covered by the time interval analyzer, which records a histogram of the time interval between consecutive pairs of photons. At low count rates, so that the average number of photocounts per 100-ns sweep is much less than 1, the time interval distribution is a good approximation to $g^{(2)}(t)$ [9]. In our system the photocount rate is typically 5 kHz so that this approximation holds. Combining the data from the time interval analyzer and the correlator then gives $g^{(2)}(t)$ over the time range ns to s.

The nature of $g^{(2)}(t)$ can be understood by considering the case of a single dye molecule in the microcavity. Figure 3 is a schematic representation of the lowest electronic energy levels of R6G. The emission of light occurs via transitions between the singlet excited state and the ground state. There is also a triplet state that the system enters and leaves nonradiatively.

$g^{(2)}(t)$ is related to the joint probability for the detection of a photon at time t_0 and the detection of a subsequent photon at some later time t_0+t. The detection of a photon at time t_0 ensures that the molecule is prepared in its ground

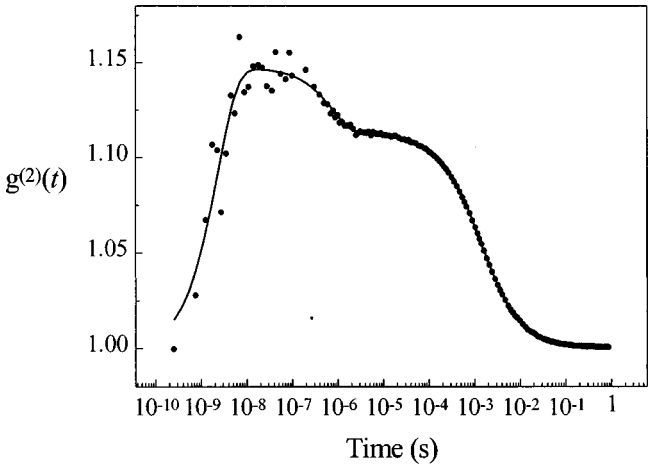

FIG. 4. $g^{(2)}(t)$ vs time for a cavity containing $10^{-8}M$ R6G and an incident laser power of 35 mW. The circles are experimental data and the line is a fit according to Eq. (23), giving the parameters $A=0.32\pm0.02$, $t_t=0.8\pm0.1$ μs, $t_e=2.3\pm0.1$ ns, $M=8.9\pm0.1$ and $t_d=1.34\pm0.07$ ms.

state. $g^{(2)}(t)$ then follows the conditioned time evolution of $\langle I_d(t_0+t)\rangle$ and hence the population of the excited singlet state.

After emitting a photon it takes a characteristic time for the electron to be excited back to the singlet excited state and to then subsequently relax emitting a second photon. This time interval is related to the excited-state lifetime and to the pumping rate and is of order ns. At short time delays, therefore, $g^{(2)}(t)$ follows the time evolution of the population of the singlet excited state and exhibits an exponential rise on a nanosecond time scale.

A further fluctuation in the signal arises from the molecule getting shelved in the triplet state. Transitions to or from the triplet state are nonradiative so that on time scales comparable to the lifetime of the triplet state there are fewer photons emitted than one would otherwise expect. This mechanism reduces the conditioned $\langle I_d(t_0+t)\rangle$ and hence we see a drop in $g^{(2)}(t)$ on time scales of order μs.

If the molecule is not fixed but is free to move within a liquid, then there is a third mechanism that gives rise to fluctuations in the fluorescence signal. The molecule can diffuse out of the collection volume under Brownian motion. For our system the diffusion time is of the order of ms and leads to a drop in the value of $g^{(2)}(t)$ on that time scale.

Figure 4 is a plot of $g^{(2)}(t)$ versus t for time scales ranging from ns to s obtained for a cavity containing $10^{-8}M$ dye solution and a laser power of 35 mW (measured at the sample). The data took one hour to accumulate. The circles are experimental points and the line is a fit to the data using Eq. (23), which is derived in the next section. The curve clearly shows the three features that we expect. The initial rise is due to antibunching, the drop at around 1 μs is due to triplet-state shelving and the drop at around 1 ms is due to diffusion. The emitted light tends, therefore, to consist of bursts of antibunched photons separated by dark intervals of orders μs due to the triplet state and ms due to diffusion.

By solving the equations that describe the dynamics of this system we now go on to derive an analytic expression for $g^{(2)}(t)$ that will allow us to extract the time constants and the number of molecules from the experimental curves.

A. Theory of number fluctuations

We can write the fluorescent intensity at time t_0 arising from a fluctuating number of molecules in a small sensing volume within a much larger sample as

$$I(t_0)=\sum_{j=1}^{N} i_j(\mathbf{r}_j,t_0), \tag{3}$$

where $i_j(\mathbf{r},t_0)$ is the intensity arising from molecule j at position $\mathbf{r}_j$ and N is the total number of molecules within the sample. The mean intensity emitted by the sample is thus

$$\langle I\rangle = N\langle i\rangle \tag{4}$$

where $\langle i\rangle$ is the intensity per molecule averaged over all positions in the collection volume. We calculate the intensity correlation function from

$$I(t_0)I(t_0+t)=\sum_{j=1}^{N} i_j(\mathbf{r}_j,t_0)\sum_{k=1}^{N} i_k(\mathbf{r}_k,t_0+t). \tag{5}$$

When we assume that emission from separate molecules is uncorrelated [10] we can separate $j=k$ terms from $j\neq k$ to obtain

$$\langle I(t_0)I(t_0+t)\rangle = N(N-1)\langle i\rangle^2 + N\langle i(t_0)i(t_0+t)\rangle. \tag{6}$$

We can write the intensity per molecule as a product of the probability of emission per unit time p and a position $\mathbf{r}$-dependent efficiency factor η describing the collection volume

$$i_j(\mathbf{r}_j,t_0)=\eta_j(\mathbf{r}_j)p_j(t_0). \tag{7}$$

In the simplest theory we assume that the molecules sit in a uniform intensity pump beam and that the averages of position and emission probability are thus separable, hence Eqs. (4) and (6) become

$$\langle I\rangle = N\langle p\rangle\langle \eta\rangle,$$

$$\langle I(t_0)I(t_0+t)\rangle = N(N-1)\langle I\rangle^2 + N\langle \eta(\mathbf{r},t_0)\,\eta(\mathbf{r}',t_0+t)\rangle \times\langle p(t_0)p(t_0+t)\rangle,$$

$$g^{(2)}(t)=\frac{N(N-1)}{N^2} + \frac{1}{N}\frac{\langle \eta(\mathbf{r},t_0)\,\eta(\mathbf{r}',t_0+t)\rangle}{\langle \eta\rangle^2}\cdot\frac{\langle p(t_0)p(t_0+t)\rangle}{\langle p\rangle^2}. \tag{8a}$$

For the diffusional case studied here we assume that N is large and in the experiment we select a small part of the sample with the optics. Equation (8a) then approximates to

$$g^{(2)}(t)=1+\frac{1}{N}\frac{\langle \eta(\mathbf{r},t_0)\,\eta(\mathbf{r}',t_0+t)\rangle}{\langle \eta\rangle^2}\cdot\frac{\langle p(t_0)p(t_0+t)\rangle}{\langle p\rangle^2}. \tag{8b}$$

We can evaluate $\langle \eta \rangle$ and $\langle \eta(\mathbf{r},t_0)\,\eta(\mathbf{r}',t_0+t)\rangle$ from

$$\langle \eta \rangle = \frac{1}{A}\int_s \eta(\mathbf{r})\,d^2\mathbf{r},$$

$$\langle \eta(\mathbf{r},t_0)\,\eta(\mathbf{r}',t_0+t)\rangle = \frac{1}{A}\int_s\int P(\mathbf{r},t_0;r',t_0+t)\,\eta(\mathbf{r})\,\eta(\mathbf{r}')\,d^2\mathbf{r}d^2\mathbf{r}'. \quad (9)$$

We assume that the probability distribution of particle position at time t_0 is uniform and $P(\mathbf{r},t_0;\mathbf{r}',t_0+t)$ is the conditional probability that the molecule found at position $\mathbf{r}$ at time t_0 is found at $\mathbf{r}'$ a time t later. The integrals are over all possible start and finish positions within the sample (total area A). When the molecule is confined to move by diffusion in two dimensions we can write [10,11]

$$P(\mathbf{r},t_0;\mathbf{r}',t_0+t) = \frac{1}{4\pi Dt}\exp\left(\frac{-(|\mathbf{r}-\mathbf{r}'|^2)}{4Dt}\right). \quad (10)$$

We then model the collection volume from which the molecular fluorescence is collected by a Gaussian function of position with $1/e^2$ half-width ω,

$$\eta(\mathbf{r}) = \eta_0\exp\left(\frac{-2|\mathbf{r}|^2}{\omega^2}\right). \quad (11)$$

Substituting Eqs. (10) and (11) into Eq. (9) we calculate the normalized correlation between the efficiencies

$$\frac{1}{N}\frac{\langle \eta(\mathbf{r},t_0)\,\eta(\mathbf{r}',t_0+t)\rangle}{\langle \eta\rangle^2} = \frac{A}{N}\frac{1}{\pi\omega^2+4Dt} = \frac{1}{\langle M\rangle}\cdot\frac{1}{(1+4Dt/\pi\omega^2)} \quad (12)$$

when we note that $N/A=C$, the concentration of molecules per unit area, and denote the average number of molecules in the scattering volume as $\langle M\rangle = C\pi\omega^2$.

B. Theory for three level molecules (R6G) in a microcavity

We now consider the fluorescence fluctuations arising from single molecules. The probability of emission at any time is going to be proportional to the steady-state probability of the molecule being in the excited singlet state $p_s(\infty)$. The detection of a photon at time t_0 [with probability $\alpha p_s(\infty)$] prepares the molecule in the ground state. The probability of emission of a second photon a time t later is then proportional to the evolution of the population of the singlet excited state conditioned on starting from the ground state $p_s(t_0,g;t)$. Hence taking the single-molecule contribution to the autocorrelation function in Eq. (8b) we can write

$$\frac{\langle p(t_0+t)p(t_0)\rangle}{\langle p\rangle^2} = \frac{p_s(t_0,g;t)}{p_s(\infty)}. \quad (13)$$

Consider the three level dye molecule shown in Fig. 3. We write the rate equations for the occupation probabilities (p_g,p_s,p_t) of the ground state, singlet excited state, and triplet states in matrix form:

$$\frac{d}{dt}\begin{pmatrix} p_g \\ p_s \\ p_t\end{pmatrix} = -\begin{pmatrix} r_{12} & -r_{21} & -r_{31} \\ -r_{12} & r_{23}+r_{21} & 0 \\ 0 & -r_{23} & r_{31}\end{pmatrix}\begin{pmatrix} p_g \\ p_s \\ p_t\end{pmatrix}. \quad (14)$$

The solutions to these equations are

$$\begin{pmatrix} p_g \\ p_s \\ p_t\end{pmatrix} = \begin{pmatrix} a_{11} & a_{12} & a_{13} \\ a_{21} & a_{22} & a_{23} \\ a_{31} & a_{32} & a_{33}\end{pmatrix}\begin{pmatrix} \exp(-\lambda_1 t) \\ \exp(-\lambda_2 t) \\ \exp(-\lambda_3 t)\end{pmatrix}, \quad (15)$$

where the λ_i are the eigenvalues of the matrix in Eq. (14), and the a_{ij} are multiples of eigenvectors, depending on the initial conditions. Diagonalizing the matrix gives

$$\lambda_1 = \tfrac{1}{2}[r_{12}+r_{21}+r_{31}+r_{23} + \sqrt{(r_{12}+r_{21}+r_{23}-r_{31})^2-4r_{12}r_{23}}],$$

$$\lambda_2 = \tfrac{1}{2}[r_{12}+r_{21}+r_{31}+r_{23} - \sqrt{(r_{12}+r_{21}+r_{23}-r_{31})^2-4r_{12}r_{23}}],$$

$$\lambda_3 = 0. \quad (16)$$

Making the approximation of low transition rates to and from the triplet state compared to the singlet excited state to ground-state decay rate, $r_{23}+r_{31}\ll r_{21}$ gives

$$\lambda_1 = r_{12}+r_{21},$$

$$\lambda_2 = r_{31}+r_{23}r_{12}/(r_{12}+r_{21}). \quad (17)$$

The $t\to\infty$ limit is of course independent of the initial conditions. The three coefficients giving equilibrium occupation probabilities are a_{13},a_{23},a_{33} and form the eigenvector corresponding to the zero eigenvalue, with the normalizing condition $a_{13}+a_{23}+a_{33}=1$. Note that $a_{23}=p_s(\infty)$. We find in the above approximation

$$a_{13} = r_{21}r_{31}/(r_{21}r_{31}+r_{12}r_{31}+r_{12}r_{23}),$$

$$a_{23} = r_{12}r_{31}/(r_{21}r_{31}+r_{12}r_{31}+r_{12}r_{23}) = p_s(\infty),$$

$$a_{33} = r_{12}r_{23}/(r_{21}r_{31}+r_{12}r_{31}+r_{12}r_{23}). \quad (18)$$

To calculate $p_s(t_0,g;t)$ we start from the initial conditions $p_g=1$, $p_s=0$, $p_t=0$ and follow the subsequent behavior of the singlet state. The remaining coefficients required are a_{21},a_{22} and they can be found from the values of p_s and dp_s/dt at $t=0$. The equations are

$$a_{21}+a_{22}+a_{23}=0,$$

$$\lambda_1 a_{21}+\lambda_2 a_{22} = -r_{12} \quad (19)$$

with solutions

$$a_{21} = -r_{12}/(r_{12}+r_{21}),$$

$$a_{22} = r_{12}^2 r_{23}/[(r_{12}+r_{21})(r_{21}r_{31}+r_{12}r_{31}+r_{12}r_{23})]. \quad (20)$$

Substituting in the appropriate part of Eq. (15) gives the results

$$p_s(t_0,g;t)/p_s(\infty)=[1-(1+a)\exp(-\lambda_1 t)+a\ \exp(-\lambda_2 t)],$$

$$\lambda_1=r_{12}+r_{21},$$

$$\lambda_2=r_{31}+r_{23}r_{12}/(r_{12}+r_{21}),$$

$$a=r_{12}r_{23}/[r_{31}(r_{12}+r_{21})]. \tag{21}$$

Substituting $p_s(t_0,g;t)$ from Eq. (21) into Eq. (13) and then combining with Eqs. (12) and (8b) we obtain the autocorrelation function,

$$g^{(2)}(t)=1+\frac{1}{M(1+4Dt/\pi\omega^2)}\times[1-(1+a)\exp(-\lambda_1 t)+a\ \exp(-\lambda_2 t)]. \tag{22}$$

Equation (22) can be reexpressed in terms of time constants rather than rate constants by making the substitutions

$$t_e=1/\lambda_1,$$

$$t_t=1/\lambda_2,$$

$$t_d=\frac{\pi\omega^2}{4D},$$

where t_e, t_t, t_d are the time constants related to the excited-state lifetime, the triplet-state lifetime, and the diffusion time, respectively. This substitution gives

$$g^{(2)}(t)=1+\frac{1}{M(1+t/t_d)}\times[1-(1+a)\exp(-t/t_e)+a\ \exp(-t/t_t)], \tag{23}$$

An interesting feature of this result is the zero-time case, $g^{(2)}(0)=1$. This means that the Poisson fluctuation in the number of molecules due to diffusion exactly cancels the intrinsic antibunching of the fluorescence from a single molecule. However, in the case where the diffusional fluctuations are frozen out $g^{(2)}(t)$ can go below one. The theory in this case requires one to use a fixed small value of N in Eq. (8a).

The theory described in this section is not correct in the situation where we have a pump intensity that varies across the volume as we have in the confocal case. However, as the diffusional fluctuations are much slower than the triplet- and singlet-state lifetimes we can calculate the single-molecule correlation function for each position in the collection volume, then perform the intensity (squared) average over all possible positions. This procedure is briefly outlined in the Appendix, where we see that at low pumping powers the general form of the correlation function is unaltered.

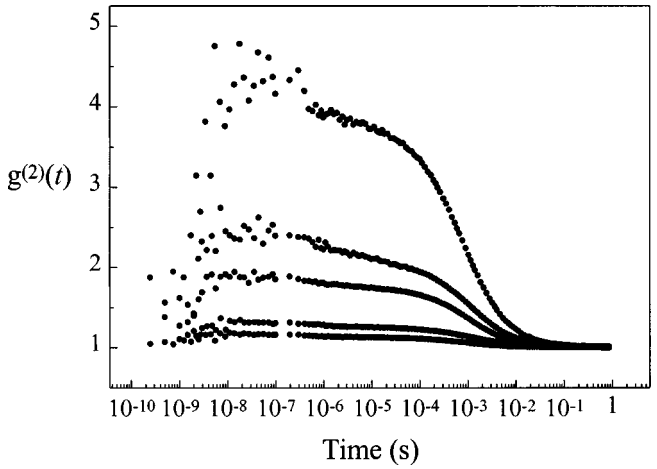

FIG. 5. Measurements of $g^{(2)}(t)$ for a range of dye concentrations between $10^{-9}M$ and $10^{-8}M$. As the dye concentration decreases the magnitude of $g^{(2)}(t)$ increases.

III. RESULTS AND DISCUSSION

The agreement between Eq. (23) and data in Fig. 4 is excellent and yields the values given in the caption. The results show the three features that we expect and because, in R6G, the three different processes occur on very different time scales we can readily determine the time constants with reasonable uncertainties. In addition, the mean number of molecules within the collection volume can also be extracted, and in this case is equal to 8.9 ± 0.1.

From Eq. (23) it is evident that the amplitude of the features in the measured value of $g^{(2)}(t)$ scale inversely with M. We can vary the number of molecules within the collection volume by changing the dye concentration. Figure 5 shows measurements of $g^{(2)}(t)$ for concentrations ranging from 10^{-9} to $10^{-8}M$ and an incident laser power of 55 mW. The lower limit on the concentration that can be used is determined by the background counts in the system. Although the measured value can be corrected for the background count rates, the uncertainties become overwhelmingly large when the photocount rate becomes smaller than the background count rate. For our system this effectively limits the concentration to being above $5\times10^{-10}M$.

Fitting Eq. (23) to the data in Fig. 5 yields the number of molecules in the collection volume as a function of dye concentration, Fig. 6. The error bars are the uncertainties arising from the fit. The straight line is a fit to the data points, forced to pass through the origin. The gradient of the line gives the effective volume of the cavity as $(1.3\pm0.1)\times10^{-18}$ m^3. This compares well with the expected value of 1.1×10^{-18} m^3 given by a 40-nm-thick dye layer and a 6-μm spot diameter. From Fig. 6 it is also apparent that we can readily reach the regime of a single dye molecule within the cavity volume by using a dye concentration of order $10^{-9}M$.

The excellent agreement between theory and data in Fig. 4 begins to break down as the laser power is increased. Figure 7 shows data recorded for a microcavity containing $10^{-8}M$ dye and an incident laser power of 90 mW. The theory and data disagree at around 10^{-5} s, with the data showing clear evidence of another fluctuation. The agreement can be restored by arbitrarily introducing another term in Eq. (23) to represent another process,

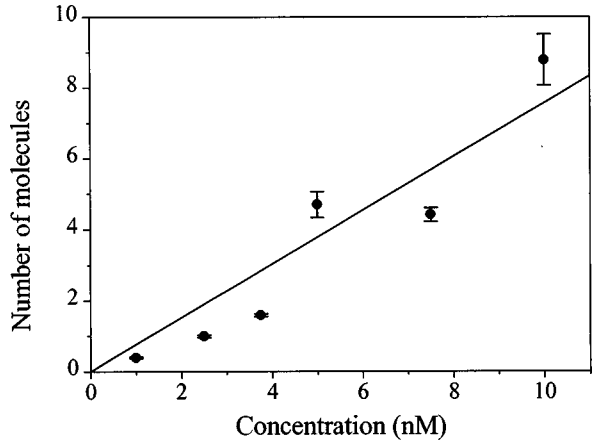

FIG. 6. The number of molecules as a function dye concentration determined by fitting Eq. (23) to the data in Fig. 5. The straight line is fit to the data points, passing through the origin.

$$g^{(2)}(t)=1+\frac{1}{M(1+t/t_d)}\left[1-(1+a+b)\exp(-t/t_e)\right.$$
$$\left.+a\ \exp(-t/t_t)+b\ \exp(-t/t_a)\right], \qquad (24)$$

where b and t_a are the amplitude and time constants, respectively, of the extra process. Equation (24) produces a good fit to the data in Fig. 7. Although it is not clear what this additional process is, there are at least two possibilities. Firstly there may be transitions to a higher energy level perhaps by two photon absorption. Alternatively, it may be a result of the fact that in the confocal arrangement the beam intensity is not uniform but will have a Gaussian profile. At high pump powers this will lead to a multiexponential triplet shelving decay (see Appendix).

By making measurements of $g^{(2)}(t)$ it is clearly possible to study the emission of light by a single molecule, and to study the fluctuations in signal that occur over a vast range of time intervals. The effect of the antibunching on the emission is seen in the dip that occurs at $t=0$. However, as noted in the theory section, $g^{(2)}(0)=1$, and this is confirmed in the experimental measurements. This is the value obtained for a classical light source, governed by Poisson statistics, so that

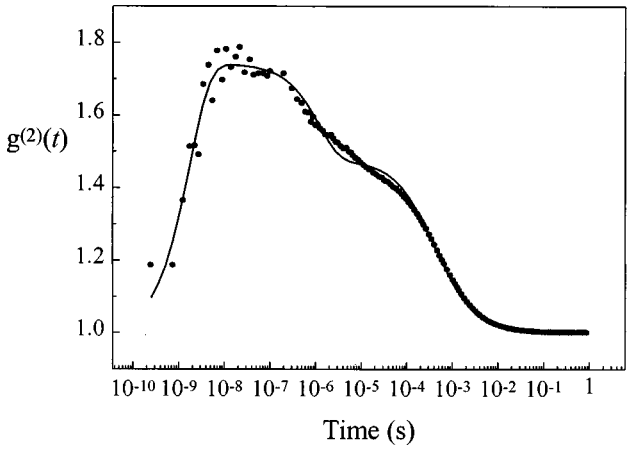

FIG. 7. $g^{(2)}(t)$ vs time for a cavity containing $10^{-8}M$ R6G and an incident laser power of 90 mW. The circles are experimental data and the line is a fit according to Eq. (23).

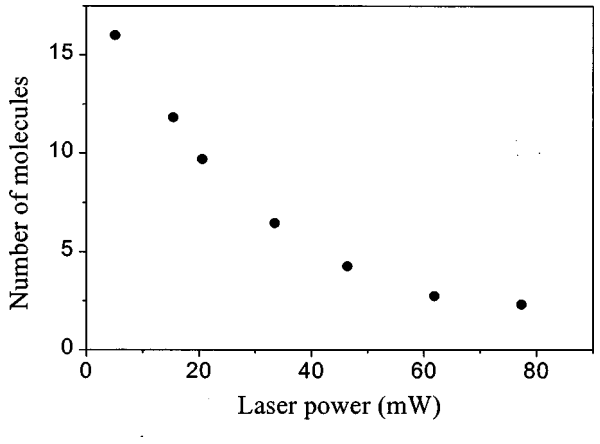

FIG. 8. The number of molecules in the collection volume as a function of the incident laser power.

the current system is no more efficient at producing single photons than a conventional attenuated laser diode. For an efficient single photon source $g^{(2)}(0)$ would be less than one and ideally would tend to zero, so that it would be impossible for two photons to be emitted at the same time. This is not the case in the current system because the number of molecules is not fixed because diffusion can take place within the liquid layer. Therefore although the average number of molecules may be one, at an instant in time there may be two or more molecules within the collection volume. It would certainly be possible to fix the number of molecules within the collection volume by immobilizing the dye layer, for instance, within a solid polymeric host. By appropriately choosing the concentration of the dye, it would be possible to arrange for there to be only one molecule within the collection volume. Organic dye molecules are, however, prone to photobleaching so such a system would have a limited lifetime.

The effect of photobleaching on our current system can be observed by making measurements of $g^{(2)}(t)$ as a function of laser power. Molecules within the intense laser beam will undergo irreversible bleaching, probably through reaction with oxygen in the solution [12]. This destruction of molecules will be balanced to some extent by diffusion of fresh molecules into the collection region. Since the pump volume is much smaller than the total cavity, a dynamic equilibrium will be reached, at least on the time scale of the measurements. The result will be a depleted number of molecules within the collection volume. As the laser power increases the photobleaching rate will also increase, resulting in a reduced equilibrium number of molecules within the cavity. If significant photobleaching occurs, it seems likely therefore, that the mean number of molecules in the cavity M will drop as the laser power increases.

Figure 8 shows the results of a series of measurements of $g^{(2)}(t)$ as a function of laser power. The graph shows the fitted value of the number of molecules as a function of the incident laser power for a $10^{-8}M$ sample. It is clear that the mean number of molecules within the collection volume does drop as the laser power increases.

The values of M were obtained by measuring $g^{(2)}(t)$ for t in the range 1 μs to 1 s, covering just the diffusional part of the full function. From Eq. (23) it is the amplitude of this

part that determines M. In order to obtain $g^{(2)}(t)$ with reasonable statistics, data was accumulated for 10 min. In order to measure $g^{(2)}(t)$ down to the small time intervals of less than 1 ns as in Figs. 4 and 7, however, data had to be accumulated for at least an hour. This was because of the relatively low photocount rates, typically 5 kHz. Although the microcavities appeared to be stable for time periods of the order of an hour, over the course of a day significant evaporation of the dye caused the cavity thickness to change. For this reason it was not possible to obtain the power dependence of $g^{(2)}(t)$ over the full time range that would have given information on the triplet state and antibunching effects.

IV. CONCLUSIONS

We have fabricated a microcavity containing a very thin layer of dye solution at the center of a $\lambda/2n$ cavity. By using a low-concentration dye solution and looking at a small volume of the cavity it is possible to reach the regime where there is only one molecule contributing to the emission. By measuring the photocount correlation function, the fluctuations in the emitted light can be simultaneously characterized over a vast range of time intervals. Fitting theory to the data gives the mean number of molecules, the diffusion time constant, the triplet lifetime, and the excited-state lifetime. Although correlation spectroscopy has been used previously to make these measurements separately [12–14], it has not previously been possible to make all these measurements over such a vast range of time scales simultaneously. We have achieved this through the simultaneous use of a digital correlator and a time interval analyzer. The potential of this technique for characterizing the photophysical properties of systems is obvious. In particular, the technique is capable of characterizing the time constants of nonradiative processes, such as triplet-state shelving and diffusion, which are difficult to extract with other techniques.

From the point of view of using individual molecules as the basis for single photon emitters the current work is encouraging. It is clearly possible to detect the light from single molecules, and to understand the kinetics of the processes giving rise to the emission. For a true single photon source, however, we need $g^{(2)}(0)=0$. In the current system this is not the case because the dye molecule number fluctuations driven by diffusion exactly balance the intrinsic antibunching from a single molecule. This could be overcome by using a solid dye layer, perhaps in a polymeric host. By applying the knowledge about triplet states and photobleaching that the current measurements are yielding together with improvements in the cavity design, it seems it may be possible to achieve an efficient source of single photon pulses using single dye molecules. Ultimately, however, the performance will be limited by photobleaching of the dye. Although this may be reduced by removing oxygen from the system and by using a more photostable dye, it may ultimately be better to use rare earth ions or quantum dots as the light sources.

ACKNOWLEDGMENTS

This work was carried out under Esprit Program No. 20029 ACQUIRE, and partially supported by the Electronics Sector of the Defence Evaluation and Research Agency. The authors are grateful to H. Rigneault of LOSCM, Ecole Nationale Supérieure de Physique de Marseille for assistance in fabricating the mirrors.

APPENDIX: THEORY FOR NONUNIFORM ILLUMINATION

We start from the general form of the correlation function given in Eq. (8b)

$$g^{(2)}(t)=1+\frac{1}{N}\frac{\langle \eta(\mathbf{r},t_0)\,\eta(\mathbf{r}',t_0+t)p(t_0)p(t_0+t)\rangle}{\langle \eta p\rangle^2}, \tag{A1}$$

but note that we cannot separate the averages when $p(t_0)$ is now also a function of $\mathbf{r}$. However, in this instance we can assume that the time scales associated with the single-molecule emission and triplet fluctuations are short compared to the diffusion component. We can thus adapt Eq. (13) to

$$\langle p(t_0+t)p(t_0)\rangle_{ts}=\langle p(\mathbf{r},t_0)\rangle_{ts}\langle p(\mathbf{r}',t_0+t)\rangle_{ts}\frac{p_s(\mathbf{r},t_0,g;t)}{p_s(\infty)}, \tag{A2}$$

where the average is taken only over short times $t_s \ll t_d$ such that $\mathbf{r}=\mathbf{r}'$ and $p_s(\infty)=\langle p(\mathbf{r},t_0)\rangle_{ts}$. From Eq. (21) we see

$$\begin{aligned}
&p_s(\mathbf{r},t_0,g;t)/p_s(\infty)\\
&\quad=[1-(1+a)\exp(-\lambda_1 t)+a\,\exp(-\lambda_2 t)],\\
&\qquad\lambda_1=r_{12}+r_{21},\\
&\qquad\lambda_2=r_{31}+r_{23}r_{12}/(r_{12}+r_{21}),\\
&\qquad a=r_{12}r_{23}/[r_{31}(r_{12}+r_{21})],
\end{aligned} \tag{A3}$$

but now the rate of excitation r_{12} is proportional to the illumination intensity. We can now substitute Eq. (A2) into Eq. (A1) and recast the long-time average over initial and final positions [Eq. (9)] as

$$\begin{aligned}
&\langle \eta p\rangle=\frac{1}{A}\int_s \langle p(\mathbf{r})\rangle_{ts}\,\eta(\mathbf{r})\,d^2\mathbf{r},\\
&\langle \eta(\mathbf{r},t_0)\,\eta(\mathbf{r}',t_0+t)p(t_0+t)p(t_0)\rangle\\
&\quad=\frac{1}{A}\int_s\int P(\mathbf{r},t_0;\mathbf{r}',t_0+t)\,\eta(\mathbf{r})\,\eta(\mathbf{r}')\\
&\qquad\times\langle p(\mathbf{r},t_0)\rangle_{ts}\langle p(\mathbf{r}',t_0+t)\rangle_{ts}\\
&\qquad\times[1-(1+a)\exp(-\lambda_1 t)+a\,\exp(-\lambda_2 t)]\\
&\qquad\times d^2\mathbf{r}\,d^2\mathbf{r}'.
\end{aligned} \tag{A4}$$

If we assume a Gaussian illumination intensity profile

$$i_p(\mathbf{r})=i_0\,\exp\left(\frac{-2|\mathbf{r}|^2}{\omega_p^2}\right) \tag{A5}$$

with $1/e^2$ width ω_p we can write the excitation rate constant as

$$r_{12}=\beta i_p(\mathbf{r}), \tag{A6}$$

and following Eq. (18),

$$p(\mathbf{r},t_0)=p_s(\infty)=a_{23}=r_{12}r_{31}/(r_{21}r_{31}+r_{12}r_{31}+r_{12}r_{23}). \tag{A7}$$

In general when r_{12} is comparable with r_{21} the integrals in Eq. (A4) can only be evaluated numerically. We can make analytic progress when $r_{12}r_{23}\ll r_{21}r_{31}$ (the weak pumping limit); then

$$\lambda_1=r_{21},$$

$$\lambda_2=r_{31},$$

$$a=r_{12}r_{23}/r_{31}r_{21}\ll 1. \tag{A8}$$

Evaluating (A4) in this limit leads to a correlation function of similar form to uniform pumping [Eq. (22)]

$$g^{(2)}(t)=1+\frac{1}{M'(1+4Dt/\omega'^2)}\times[1-(1+a')\exp(-\lambda_1 t)+a'\ \exp(-\lambda_2 t)] \tag{A9}$$

with a modified mean number of molecules arising from a reduction in the effective beam waist to $\omega'=\omega\omega_p/\sqrt{\omega^2+\omega_p^2}$ and a modified triplet shelving fraction

$$a'=\frac{\beta i_0 r_{23}(\omega^2+\omega_p^2)}{r_{31}r_{21}(3\omega^2+2\omega_p^2)}. \tag{A10}$$

In the case of ideal confocal pumping $\omega=\omega_p$; then $\omega'=\omega/\sqrt{2}$ and $a'=2\beta i_0 r_{23}/5r_{31}r_{21}$. The above approximations are only valid when $a<0.1$, which is clearly not the case for the data presented. We may thus ask why the results fit the simple model so well when $a\approx 0.3$. It is clear, even for the maximum pumping rate we have achieved, that $r_{12}\ll r_{21}$. In this case

$$\lambda_1=r_{21},$$

$$\lambda_2=r_{31}(1+a),$$

$$a=r_{12}r_{23}/r_{31}r_{21}. \tag{A11}$$

The integral in Eq. (A4) now involves averaging over the Gaussian distributed linewidth λ_2. It is well known that distributions of exponentials with up to 30% width are difficult to distinguish from a single exponential decay without very low noise data. Hence we are not surprised that the data continue to fit the simple model up to $a\approx 0.3$. However, at the highest pumping powers we might expect to see the triplet shelving decay become multiexponential as in Fig. 7.

[1] Th. Basché, W. E. Moerner, M. Orrit, and H. Talon, Phys. Rev. Lett. **69**, 1516 (1992).

[2] W. P. Ambrose, P. M. Goodwin, J. C. Martin, and R. A. Keller, Science **265**, 364 (1994).

[3] U. Mets and R. Rigler, J. Fluoresc. **4**, 259 (1994).

[4] C. H. Bennett, F. Bessette, G. Brassard, L. Salvail, and J. Smolin, J. Cryptology **5**, 3 (1992); P. D. Townsend, J. G. Rarity, and P. R. Tapster, Electron. Lett. **29**, 634 (1993).

[5] H. J. Kimble, M. Dagenais, and L. Mandel, Phys. Rev. Lett. **39**, 691 (1977).

[6] F. De Martini, G. Di Giuseppe, and M. Marrocco, Phys. Rev. Lett. **76**, 900 (1996).

[7] E. L. Elson and D. Magde, Biopolymers **13**, 1 (1974).

[8] F. T. Arecchi, M. Corti, V. Degiorgio, and S. Donati, Opt. Commun. **3**, 284 (1971).

[9] S. Chopra and L. Mandel, Rev. Sci. Instrum. **43**, 1489 (1972).

[10] P. N. Pusey, in *Photon Correlation and Velocimetry*, edited by H. Z. Cummins and E. R. Pike (Plenum, New York, 1976), p. 45.

[11] S. Chandrasekar, Rev. Mod. Phys. **15**, 1 (1943).

[12] J. Widengren and R. Rigler, Bioimaging **4**, 149 (1996).

[13] U. Mets, J. Widengren, and R. Rigler, Chem. Phys. **218**, 191 (1997).

[14] J. Widengren, R. Rigler, and U. Mets, J. Fluoresc. **4**, 255 (1994).